



Title: **Physical and chemical properties using commercial diesel and palm oil biodiesel blends**



Authors: Oscar Hernando Venegas-Pereira, Luisa Fernanda Mónico-Muñoz

DOI: **10.17533/udea.redin.20250258**

To appear in: *Revista Facultad de Ingeniería Universidad de Antioquia*

Received: February 22, 2024

Accepted: February 20, 2025

Available Online: February 21, 2025

This is the PDF version of an unedited article that has been peer-reviewed and accepted for publication. It is an early version, to our customers; however, the content is the same as the published article, but it does not have the final copy-editing, formatting, typesetting and other editing done by the publisher before the final published version. During this editing process, some errors might be discovered which could affect the content, besides all legal disclaimers that apply to this journal.

Please cite this article as: O. H. Venegas-Pereira, L. F. Mónico-Muñoz. Physical and chemical properties using commercial diesel and palm oil biodiesel blends, *Revista Facultad de Ingeniería Universidad de Antioquia*. [Online]. Available: <https://www.doi.org/10.17533/udea.redin.20250258>



Physical and chemical properties using commercial diesel and palm oil biodiesel blends Propiedades físicas y químicas usando mezclas comerciales de diésel y biodiésel de aceite de palma

Oscar Hernando Venegas-Pereira¹ <https://orcid.org/0000-0001-6903-4100> Luisa Fernanda Mónico-Muñoz^{2*}
<https://orcid.org/0000-0002-3597-6332>

Programa de Ingeniería Mecánica, Escuela Colombiana de Ingeniería Julio Garavito. AK. 45 # 205 – 59 Autopista Norte. C. P. 111166. Bogotá D.C., Colombia.

Programa de Ingeniería Aeronáutica, Fundación Universitaria Los Libertadores. Carrera 16 # 63 A – 68. C. P. 111221. Bogotá D.C., Colombia

Corresponding author: Luisa Fernanda Mónico-Muñoz

E-mail: luisa.monico@libertadores.edu.co

KEYWORDS

Biodiesel; commercial diesel; physical properties; chemical properties

Biodiesel, diésel, propiedades físicas, propiedades químicas

ABSTRACT: In different studies on the impact of fuel blends on the performance and polluting emissions of an internal combustion engine, it is necessary to identify some physical and chemical properties that allow understanding of the behavior of the results; however, obtaining such properties requires the use of special equipment that may incur additional costs. In this document, from some experimental tests, it has been possible to obtain the behavior of physical and chemical properties (density, boiling temperature, cetane index, kinematic viscosity, heat values, and adiabatic flame temperature) for different commercial diesel and palm oil Biodiesel blends. Additionally, the data obtained were statistically treated to obtain fit equations that predict the behavior of most of the properties studied for blend percentage values different from those tested.

RESUMEN: En diferentes estudios sobre el impacto de las mezclas de combustibles en el rendimiento y emisiones contaminantes de un motor de combustión interna, es necesario conocer algunas propiedades físicas y químicas que permitan comprender el comportamiento de los resultados; sin embargo, obtener dichas propiedades requiere el uso de equipos especiales que pueden generar costos adicionales. En este documento, a partir de algunas pruebas experimentales, se ha podido obtener el comportamiento de las propiedades físicas y químicas (densidad, temperatura de ebullición, índice de cetano, viscosidad cinemática, poder calorífico y temperatura de llama adiabática) para diferentes mezclas de diésel comercial y Biodiésel de aceite de palma. Adicionalmente, los datos obtenidos fueron tratados estadísticamente para obtener ecuaciones de



ajuste que permitan predecir el comportamiento de la mayoría de las propiedades estudiadas para mezclas de diferentes valores porcentuales.

1. Introduction

In recent years, different industries worldwide have had to face and started implementing solutions to all the environmental issues that have arisen over time, mainly due to the use of fossil fuels [1]. Over the years, the use of vehicles has increased, leading to an increase in the demand for fuel derived from petroleum [2]. This combustion produces high amounts of greenhouse gases and acid rain [3]. Diesel engines have the advantage of being more efficient and, thus, emit less CO₂ than gasoline engines; however, they produce high levels of NO_x and particulates, which cause negative effects on people's health, as well as the environment [4].

Various alternatives have been proposed to address these difficulties, including the use of alternative fuels such as Biodiesel. The indiscriminate burning of fossil fuels has been shown to be the main reason for high pollution levels in cities. This is evidenced by the accumulation of particles in the form of a smog cloud, as well as the formation of acid rain and an increase in greenhouse gases. Biodiesels stand out for their ease of use, production, and storage. They are considered less toxic and more biodegradable; they also have low sulfur content and the potential to reduce particulate matter, CO, HC, and CO₂ levels [5] [6] [7] [8] [9].

At the national level, in 2023 Colombia mainly produced bioethanol from sugar cane and Biodiesel from palm oil, with a monthly national demand of approximately 25,000,000 liters and 54,000 tons, respectively [10]. However, in recent years, the development of projects has been promoted, among which is the operation of the first alcohol production plant from cassava [11] [12]. Projects with sugar beets or with sugar cane, unfortunately, have not been able to advance because of the international financial crisis [13] [14]. These works on biofuels are an example of the actions that can be developed to contribute to the care of the environment.

Many studies have strengthened the analysis of the performance trends and polluting emissions obtained in engines with the physical properties of the fuels tested [15]. For example, density is an easily measured property that can be correlated with other properties to assess the performance of fuels used in compression ignition engines, such as heating value and cetane number.

In the literature, it is possible to find equations that provide an idea of the various physicochemical properties of fuels or blends tested in different engines as substitutes for conventional fuels. In another investigation, a set of base parameters for the evaluation of Biodiesel was obtained through a simulation of the processes in Matlab. This study used descriptive statistical methods, sampling, as well as correlation and mathematical methods such as least squares, linear, and exponential applications, among others, to generate a joint analysis of the information, as well as the models used, achieving a greater degree of accuracy and confidence in the studies. The data obtained from the simulation of the



physicochemical properties were close to the experimental values reported in the literature, which allowed their use [16].

For calculating the density for palm oil biodiesel and its 5% and 20% blends with conventional petroleum derived diesel fuel (BACP- ACPM) a simple mixing law (weighted mass average) was proposed leading to absolute maximum deviations lesser than 0.5% of measured data [17]. Likewise, empirical correlations, like Andrade equation, have also been presented to predict the effect of temperature on the absolute and kinematic viscosity of palm oil Biodiesel. They obtained a correlation to determine the viscosity at 40°C of the blends depending on the amount of Biodiesel in the blend [18].

In the study by [19], a bibliographic compendium related to the equations used to calculate the properties of biofuel blends was prepared. A methodology based on equations known as "mixing rules" was included to estimate the physicochemical properties of Biodiesel with petroleum diesel from four raw materials: palm oil, sunflower oil, jatropha oil, and pork fat. Density, viscosity, cloud point, cetane number, heat capacity, API gravity, and vapor pressure were analytically estimated for different Biodiesel-Diesel blends.

The aim of this work is to determine the behavior of density, boiling temperature, cetane index, kinematic viscosity, high and low heat values, and adiabatic flame temperature for different commercial diesel and palm oil Biodiesel blends. It also seeks to establish fitting equations that allow easy determination of the value of some physical and chemical properties for different concentrations of Biodiesel from those tested, which would help reduce time and costs in studies related to this biofuel.

2. Methodology

Based on the type of research conducted and the procedures used to obtain results, it was determined that the methodology proposed in this research project was strictly experimental. For the development of this project, two types of fuels were used to prepare different blends: palm oil Biodiesel (B100) and commercial Diesel (B10). Subsequently, considering that commercial Diesel contains 10% palm oil biofuel, the volume amount of B100 to be added to obtain B25, B50, and B75 was calculated (the number indicates the amount of palm oil Biodiesel in volume).

ASTM D1398 and ASTM D446 standards were used for the density and kinematic viscosity tests, respectively. For each of the five fuels (B10, B25, B50, B75, and B100), the density and kinematic viscosity were measured in the temperature range of 20°C to 80°C, and the temperature was varied using a thermostatic bath with increments of 10°C. The cetane index was calculated using the ASTM D976 standard, for which it is necessary to obtain distillation curves following the ASTM D86-12 standard using a manual Distillation Analyzer. A heating value test for each blend was performed in accordance with the ASTM D 240 standard.



On the other hand, considering the gas chromatography carried out by the Biodiesel manufacturer (see Table 1), a stoichiometric balance was made to determine the higher and lower heating values and adiabatic flame temperature for each blend.

Table 1. Composition of Biodiesel B100 given by the manufacturer

Compound	Formula	Composition [%mol]
Myristic acid	$C_{14}H_{28}O_2$	0.75
Palmitic acid	$C_{16}H_{32}O_2$	38.91
Stearic acid	$C_{18}H_{36}O_2$	4.22
Oleic acid	$C_{18}H_{34}O_2$	45.51
Linoleic acid	$C_{18}H_{32}O_2$	10.03
Linolenic acid	$C_{18}H_{30}O_2$	0.22
Arachidic acid	$C_{20}H_{40}O_2$	0.36

Additionally, the manufacturer carried out an analysis of Fatty Acid Methyl Ester (FAME) to corroborate the percentage of biofuel in the commercial fuel and in each blend made, as presented in **Table 2**. From the table, it is observed that the commercial fuel contains approximately 10% of biofuel, and that the other blends have a value in line with the desired value sought during the manufacture of each one.

Table 2. FAME of used fuels

Fuel	FAME [%]
B10	9.6
B25	25.4
B50	49.8
B75	75.4
B100	99.8

3. Results

This section presents the experimental results that helped define the fit models for each of the analyzed fuel properties. For each fitting model, the average value of each property under study was taken, and the StatGraphics software was used to find the coefficients for each of the proposed fittings.

3.1. Density

Measurements are taken by keeping the bath at a stable temperature, and then the density and temperature are measured according to the standard. Subsequently, the temperature changes and the thermostatic bath is set to target temperatures of 20°C, 40°C, 60°C and 80°C. The precision error associated with the measuring element is 0.5 kg/m³.

Table 3. Experimental density data



Fuel	Density [kg/m ³]	Bath Temperature [°C]
B10	859	20
	846	40
	831	60
	818	80
B25	859	20
	846	40
	832	60
	820	80
B50	864	20
	850	40
	837	60
	823	80
B75	868	20
	854	40
	840	60
	826	80
B100	872	20
	858	40
	843	60
	830	80

Using the results obtained experimentally, a regression was statistically determined, which allowed an estimate of the density values at different concentrations between the BioD palm oil Biodiesel and the commercial diesel used at different temperatures. Therefore, the expression presented in Equation 1 relates the amount in volume of Biodiesel in the blend (%Bio), the temperature at which it is needed to calculate the density (T), and the constants A, B, C, D and E, which are tabulated in **Table 4**, according to the statistical estimate. The expression proposed is shown in Equation (1) and subsequently, entering this equation into Statgraphics, each of the coefficients is obtained, verifying that they are statistically representative.

$$\rho = [A \cdot \tanh(B + 100 - \%Bio) - 1.5] \cdot T + 1000 - C \cdot \tanh\left(\frac{D+100-\%Bio}{E}\right) \quad (1)$$

Table 4. Density estimation results by the Marquardt method

Constant	Value	Standard error asymptotic	Confidence interval	
			Higher	Lower
A	0.807981	0.00920693	0.787717	0.828245
B	1.84539	0.241354	1.31417	2.37661



C	135.697	4.03684	126.812	144.582
D	197.021	47.1697	93.2009	300.841
E	165.636	48.1925	59.5646	271.707

Table 4 shows that the constants obtained statistically from the expression do not contain zero in the confidence interval (95%); therefore, the coefficients are statistically representative of the fit equation (Equation 1) with a standard deviation of the residuals of 0.70.

As shown in **Figure 1**, the density obtained experimentally decreases as the temperature increases linearly, according to theory. Additionally, it was observed that a higher Biodiesel content in the blend led to higher density values. The point called BioD corresponds to the value delivered by the biofuel manufacturer, which has a value of 875.6 kg/m³ at 15°C and corresponds to the trend of B100, although the tests were carried out at 20°C.

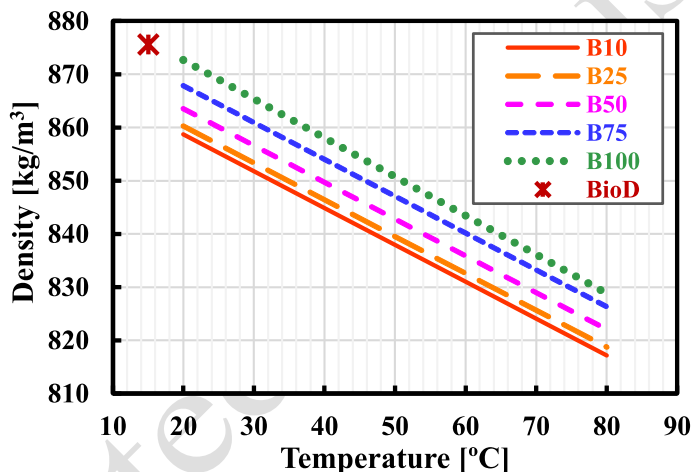


Figure 1. Density of the fuels at different temperatures

3.2. Distillation curves

Distillation is a physical separation process based on the difference in the volatility of various blends or solution components. The objective is to separate the different components based on the differences in their boiling points. A distillation curve was obtained by collecting the distilled volume at a given temperature. The precision error associated with the measuring elements is 0.5 % for distilled volume and 0.5°C for boiling temperature.

Figure 2 shows the distillation curves obtained for each fuel. As the amount of Biodiesel in the blend increases, the temperatures reached are higher. With the values of the temperature obtained for 50% of the distillate volume and the density of each blend, it is possible to calculate the estimated value of the cetane index, as will be presented later.

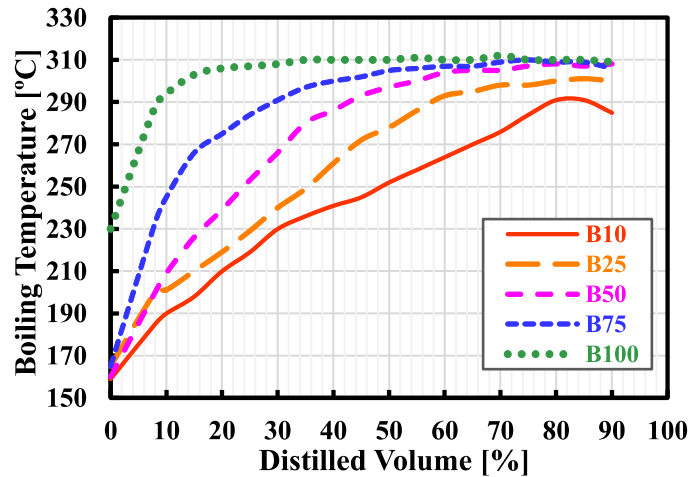


Figure 2. Distillation curves for each fuel

In **Figure 3**, it can be seen how the boiling temperature varies for 50% of the distilled volume depending on the percentage of biofuel, reaching a correlation (Equation 2) with an adjustment of 99.69%, which allows the determination of the boiling temperature point for 50% of the distilled volume of different blends from those used in this study.

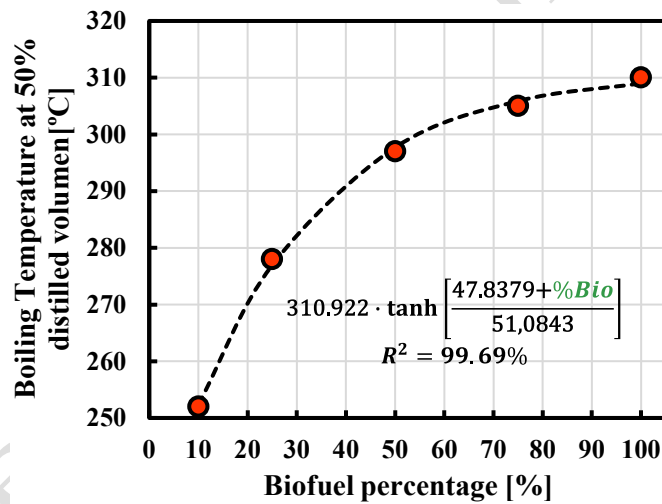


Figure 3. Boiling temperature at 50% distilled volume

$$B = 310.922 \cdot \tanh \left[\frac{47.8379 + \%Bio}{51.0843} \right] \quad (2)$$

3.3. Cetane index

Cetane index is a measure of the fuel ignition quality; that is, it indicates the ignition ability under the temperature and pressure conditions of the engine combustion chamber [20]. It is a theoretical approximation of the cetane number and is calculated from the density and distillation rate of the fuel. On the other hand, the cetane number is a standardized laboratory test, which is determined by comparing the behavior of the fuel tested with two reference mixtures with the known cetane number. In the studies by [21] [22], a comparison between the cetane number and cetane index can be seen. Normally, the cetane index is used to analyze the delay times, which can be estimated from the distillation curve and

density of the fuel [23]. The cetane index was calculated using the ASTM D976 standard [24], using equation 3:

$$IC = 454.74 - 1641.416D + 774.74D^2 - 0.554B + 97.803(\log B)^2 \quad (3)$$

where

D = sample density at 15°C in g/mL

B = boiling temperature for 50% of the distilled sample (°C) (Equation 1).

The cetane index values are shown in **Figure 4**. According to the data obtained, it can be stated that as the percentage of Biodiesel in the blend increases, the cetane index increases. It should be noted that in the case of fuels B75 and B100, the values obtained from the cetane index have very similar results. This is because it is a function of the density and boiling temperature of 50% of the distillate volume, and for these two fuels, these values do not present significant variations, as presented in **Figure 1** and **Figure 3**.

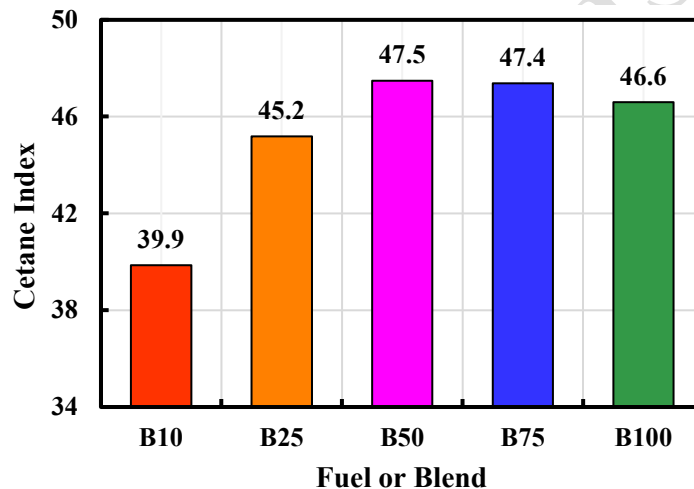


Figure 4. Cetane index for each fuel.

Additionally, because there is an equation that allows the calculation of the density based on the percentage of Biodiesel in the blend and the boiling temperature for 50% of the distilled volume, it was possible to establish an expression that related the amount of Biodiesel in the blend with the boiling temperature. This made it possible to have an estimate of the cetane index. This expression is given by Equation 4.

$$IC = 454.74 - 1641.416D + 774.74D^2 - 0.554T + 97.803(\log T)^2 \quad (4)$$

where

D = sample density at 15°C in g/mL

T = boiling temperature (°C) for 50% of the distilled sample (°C.) (Equation 1).

3.4. Higher heating value

The higher heating value is the maximum amount of heat that can be obtained from the products of complete combustion if those products are cooled to the original temperature of the air-fuel mixture and

the water generated is condensed. Heating value mainly depends on the amount of water vapor that condenses during the cooling of products after combustion. The heating value is always measured per unit mass or unit volume of oxidized fuel. The water vapor is generated during combustion due to the reaction of hydrogen present in the fuel composition and humidity adhered to the fuel itself [25].

For this test, a Mettler Toledo analytical balance model AB 204 SNR 111660708 (Switzerland) and an IKA C 2,000 Basic S1 Calorimeter operating in Isoperibolic mode were used. Grade 2.7 extra-dry industrial oxygen at a pressure of 30 bar was used. The temperature of the calorimeter jacket was maintained at 25°C using a Julabo F12 thermostatic bath. Test results are presented in **Figure 5**, where increasing the percentage of Biodiesel in the blend decreased the calorific value. The Calorific value test for each of the blends to be tested was performed at the Chemical Engineering Laboratory of the Universidad Nacional in accordance with the ASTM D 240 standard, as mentioned earlier.

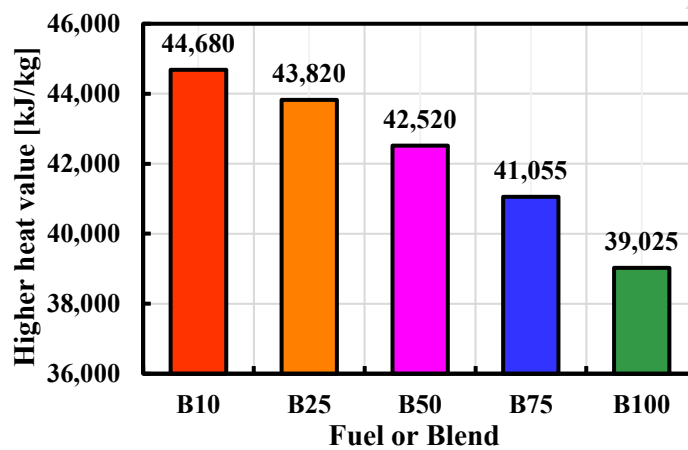


Figure 5. Higher heat value for each fuel

3.5. Kinematic viscosity

The kinematic viscosity is the ratio of dynamic viscosity to fluid density. In this case, viscosity is the resistance of a fluid to slip, which depends on the nature of the liquid and temperature. To analyze this property, the variation of viscosity with temperature (from 20°C to 80°C) was experimentally measured. **Table 5** shows the results obtained for average viscosity measurement at different temperatures for each of the tested fuels with the standard deviation.

Table 5. Average experimental data of viscosity

Fuel	Average viscosity [cSt]	Standard deviation [cSt]	Bath Temperature [°C]
B10	6,765	0,030	20
	4,015	0,083	40
	2,601	0,018	60
	1,884	0,008	80
B25	6,472	0,080	20
	3,804	0,085	40
	2,565	0,000	60

	1,830	0,014	80
B50	6,661	0,091	20
	4,050	0,047	40
	2,761	0,027	60
	2,019	0,008	80
	7,119	0,095	20
B75	4,294	0,025	40
	2,810	0,024	60
	2,117	0,008	80
	7,192	0,133	20
B100	4,340	0,006	40
	3,042	0,024	60
	2,215	0,009	80

To have a theoretical approximation, an expression was established that relates, as in the case of density, the temperature at which it is required to determine this property, and the percentage of Biodiesel in the blend, resulting in Equation 5.

$$v = (A + B \cdot T) \cdot \%Bio + 10 - C \cdot \tanh\left(\frac{D+T}{E}\right) \quad (5)$$

Where

%Bio = the percentage of Biodiesel in the blend.

T = the temperature at which viscosity is required to be calculated (T)

A, B, C, D and E = constants. They are presented in **Table 5** according to the statistical estimate.

The results of said expression were compared with the data obtained experimentally, resulting in a confidence interval of 95.0% with a standard deviation of the residuals of 0.12. As shown in **Figure 6**, the viscosity obtained experimentally decreases as the temperature increases exponentially, according to theory.

Table 6. Kinematic viscosity estimation results by the Marquardt method

Constant	Value	Standard error asymptotic	Confidence interval	
			Higher	Lower
A	0.00868046	0.0021426	0.0133963	0.00396463
B	-0.0000639141	0.0000392503	0.0000224755	-0.000150304
C	8.53648	0.144258	8.85399	8.21897
D	-2.42404	0.980345	-0.266308	-4.58177
E	41.1935	2.32722	46.3157	36.0713

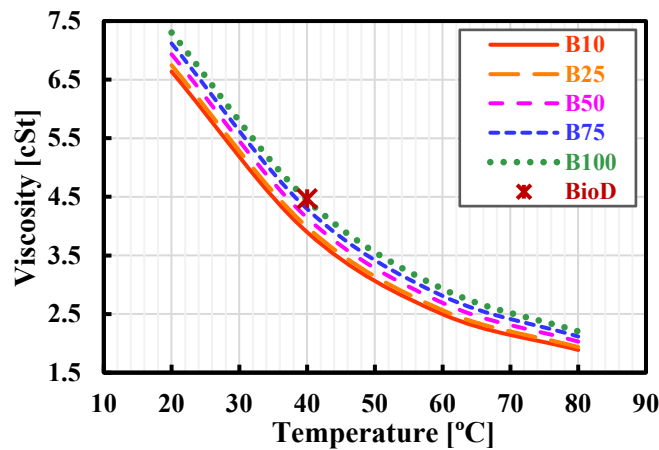


Figure 6. Viscosity of the fuels at different temperatures.

In **Table 6**, a summary of the main properties of each of the established blends is presented.

Table 7. Basic properties of used fuels

Fuel	Density [kg/m ³]	Cetane Index	Higher heat value [kJ/kg]	Viscosity 40°C [cSt]
B10	862.1	39.855	44,680	3.896
B25	863.7	45.181	43,820	3.988
B50	867.0	47.474	42,520	4.141
B75	871.3	47.367	41,055	4.294
B100	876.3	46.591	39,025	4.448

3.6. Stoichiometric balance and higher and lower heating value

After characterizing the different physical and chemical properties of the fuel blends, a study of the stoichiometric balance was carried out to analytically obtain the higher and lower calorific value for the different fuels. The actual fuel is composed of many hydrocarbons whose presence and proportion varies depending on the origin of the crude. Fuel production is a function of the refining process, legislative requirements, among others. The above affects the exact composition of the fuel, and therefore its effect on combustion. One option is to work with substitute fuels, which reproduce the chemical and physical properties of the fuel and are much easier to analyze [26].

In many studies carried out [27], [28], [29], dodecane ($C_{12}H_{26}$) has typically been used for Diesel fuel, although in other studies multi-component replacement fuels have been developed [30], [31]. In the case of Biodiesel derived from vegetable oils (rapeseed, sunflower, soy, palm, among others), they generally involve more than 50% saturated fatty acids and less than 5% Poly- Unsaturated Fatty Acids. For the biofuel from palm oil, **Table 7** shows the composition of the replacement fuel, together with the molar percentage and the enthalpy of formation of each component. This shows that the values obtained in gas chromatography for Biodiesel Premium Gold are consistent in orders of magnitude with what is found in theory. From here on, we work with the values obtained by gas chromatography.

Table 8. Composition of Biodiesel from Palm Oil [32] [33, 34]



Compound	Formula	Manufacturer [%mol]	Literature [%mol]	$\Delta \bar{h}_f^\circ$ [kJ/kmol]
Myristic acid	$C_{14}H_{28}O_2$	0.75	1	-834,100
Palmitic acid	$C_{16}H_{32}O_2$	38.91	44	-848,400
Stearic acid	$C_{18}H_{36}O_2$	4.22	6	-891,000
Oleic acid	$C_{18}H_{34}O_2$	45.51	38	-764,800
Linoleic acid	$C_{18}H_{32}O_2$	10.03	10	-634,700
Linolenic acid	$C_{18}H_{30}O_2$	0.22	0.5	-508,800
Arachidic acid	$C_{20}H_{40}O_2$	0.36	0.5	-1,012,600

Knowing the real composition of the Biodiesel used in the tests, it is possible to carry out the stoichiometric analysis for each of the fuels under study (B10, B25, B25, B50, and B100), taking into account the percentage in moles of biofuel given in **Table 8**, in order to obtain the higher and lower heating value of each fuel.

Table 9. Percentage of biofuel in volume, mass and molar for each blend

Fuel	%Volume	%Mass	%Moles
B10	9.6	9.74	6.56
B25	25.0	25.31	18.07
B50	50.0	50.41	39.82
B75	75.0	75.30	66.50
B100	100.0	100.00	100.00

The approach carried out for B10 is shown below; for the other fuels, it is carried out in a similar way.

$$0.066 \cdot (0.008 \cdot C_{14}H_{28}O_2 + 0.39 \cdot C_{16}H_{32}O_2 + 0.04 \cdot C_{18}H_{36}O_2 + 0.46 \cdot C_{18}H_{34}O_2 + 0.1 \cdot C_{18}H_{32}O_2 + 0.002 \cdot C_{18}H_{30}O_2 + 0.004 \cdot C_{20}H_{40}O_2) + 0.934 \cdot C_{12}H_{26} + A \cdot (O_2 + \frac{79}{21} \cdot N_2) \rightarrow B \cdot CO_2 + D \cdot H_2O + E \cdot N_2$$

Carrying out the balance (CHON) we obtain:

$$C: 0.066 \cdot [0.008 \cdot (14) + 0.39 \cdot (16) + 0.04 \cdot (18) + 0.46 \cdot (18) + 0.1 \cdot (18) + 0.002 \cdot (18) + 0.004 \cdot (20)] + 0.934 \cdot (12) = B$$

$$H: 0.066 \cdot [0.008 \cdot (28) + 0.39 \cdot (32) + 0.04 \cdot (36) + 0.46 \cdot (34) + 0.1 \cdot (32) + 0.002 \cdot (30) + 0.004 \cdot (40)] + 0.934 \cdot (26) = 2 \cdot D$$

$$O: 0.066 \cdot [0.008 \cdot (2) + 0.44 \cdot (2) + 0.06 \cdot (2) + 0.38 \cdot (2) + 0.1 \cdot (2) + 0.005 \cdot (2) + 0.005 \cdot (2)] + 2 \cdot (A) = 2 \cdot B + D$$

$$N: 2 \cdot (\frac{79}{21}) \cdot A = 2 \cdot E$$

Solving the system of equations, we get:

$$B = 12.34 \text{ kmol}$$



$$D = 13.23 \text{ kmol}$$

$$A = 18.89 \text{ kmol}$$

$$E = 71.07 \text{ kmol}$$

Having the system solved, the air-fuel ratio (A/F) for B10 is determined.

$$M_{B10} = 176.66 \text{ kg/kmol}$$

$$\text{kmol air} = A \cdot (1 + 79/21) = 89.93 \text{ kmol}$$

$$\frac{A}{F} = \frac{89.96 \text{ kmol} \cdot (28.84 \text{ kg/kmol})}{1 \text{ kmol} \cdot (176.66 \text{ kmol/kmol})} = 14.69 \text{ kg}_{\text{air}}/\text{kg}_{\text{fuel}}$$

The higher and lower heating values are now determined from the enthalpy of reaction at reference conditions, taking into account the values of the enthalpy of formation of the components given in **Table 9**, including that of dodecane ($C_{12}H_{26}$).

Table 10. Formation enthalpies of different compounds

Name	$\Delta \bar{h}_f^o$ [kJ/kmol]
H_2O (liquid)	-285,830
H_2O (gas)	-241,826
CO	-110,527
CO_2	-393,522
NO	90,291
NO_2	33,095
$C_{12}H_{26}$	-352,100

$$\Delta H_c = \sum_{\text{products}} N_p \cdot \Delta \bar{h}_f^o - \sum_{\text{reactants}} N_r \cdot \Delta \bar{h}_f^o$$

$$\Delta H_c (H_2O \text{ liquid}) = Q_{HV} = \left| -46,744.18 \text{ kJ/kg}_{\text{fuel}} \right|$$

$$\Delta H_c (H_2O \text{ gas}) = Q_{LV} = \left| -43,448.21 \text{ kJ/kg}_{\text{fuel}} \right|$$

Table 10 summarizes the values obtained for all the fuels under study.

Table 11. Calculated higher and lower heat value

Fuel	A/F [-]	Q_{HV} [kJ/kg _{fuel}]	Q_{LV} [kJ/kg _{fuel}]
B10	14.69	46,744.18	43,448.21
B25	14.28	45,446.59	42,259.83
B50	13.63	43,386.86	40,373.45
B75	12.99	41,382.93	38,538.19



B100	12.38	39,432.58	36,751.98
------	-------	-----------	-----------

When comparing the results of the higher heating value, those obtained in the laboratory under the ASTM 240 Standard with those obtained analytically, a maximum error of 4.6% is found for B10 (see **Table 11**). The above demonstrates that the composition of the biofuel found through chromatography together with the stoichiometric analysis, allows us to have an approximate value of the heating value of the fuel of any mixture between Biodiesel and commercial Diesel. In a later study, the error found could be reduced by working with a replacement fuel for commercial Diesel with properties closer to the Diesel produced and marketed in Colombia.

Table 12. Comparison between standard and analytical higher heat value

Fuel	ASTM 240 [$\text{kJ}/\text{kg}_{fuel}$]	Analytical [$\text{kJ}/\text{kg}_{fuel}$]	Error [%]
B10	44,680	46,744.18	4.6
B25	43,820	45,446.59	3.7
B50	42,520	43,386.86	2.0
B75	41,055	41,382.93	0.8
B100	39,025	39,432.58	1.0

3.7. Adiabatic Flame Temperature

The combustion of any fossil fuel produces a certain level of NO_x due to the high temperatures and the availability of oxygen and nitrogen. These NO_x emissions generated in the combustion processes are made up of approximately 95% NO and the rest NO_2 . According to [35], in the Diesel combustion process, the formation of NO occurs in the last phase of combustion (diffusion combustion) due to the high temperature (above $1,200^\circ\text{C}$) that generates the formation of NO_x .

Studies such as [36], [37], [38], [39], [40], have used low temperature combustion (LTC) strategies in order to achieve combustion in a diesel engine cleaner in terms of NO_x and soot emissions thanks to the reduction of the adiabatic flame temperature in the combustion chamber. In accordance with the above, in this section, it is intended to demonstrate the effect of the maximum combustion temperature on the formation of NO_x in each of the tested points. To do this, the operating conditions of the engine will be considered, such as the coefficient of excess air (greater than unity at all points due to supercharging), engine temperature, and environmental conditions (moisture present in the air sucked in by the engine). With NO and CO_2 measurements and working with the replacement fuels studied in the previous section, the real balances (CHON) are carried out again.

Additionally, using the analytical methodology from the previous section, it is possible estimate enthalpy as a function of the temperature of different components [33]. The reaction enthalpy must be considered to determine the maximum combustion temperature reached at each point, equaling the reaction enthalpy to zero, indicating that all the energy of the reactants passes entirely to the products without loss to the outside.



$$\Delta H_c = \sum_{products} N_p \cdot (\Delta \bar{h}_f^o + \bar{h} - \bar{h}^o) - \sum_{reagents} N_r \cdot (\Delta \bar{h}_f^o + \bar{h} - \bar{h}^o) = 0$$

$$\text{where, } \bar{h} - \bar{h}^o = A \cdot T + B \cdot T^2/2 + C \cdot T^3/3 + D \cdot T^4/4 - \frac{E}{T} + F - H$$

The value of the coefficients (A to H) is also obtained from [33] for each of the components. It is assumed that the fuel enters the reaction at 25°C, and the air enters the chamber at a temperature close to the engine temperature for each test point. Therefore, when the enthalpy of the reaction is equal to zero, the only unknown data is the temperature at the exit of the products. This temperature is the one reached in combustion and is found iteratively.

Figure 7 shows the behavior of the calculated combustion temperature for each of the operating conditions and each of the blends. In general, it is observed that, for the different blends, the temperature range at all load degrees and operating regimes remain between 800 K and 1,700 K, with slight differences in their behavior as the rotation regime increases.

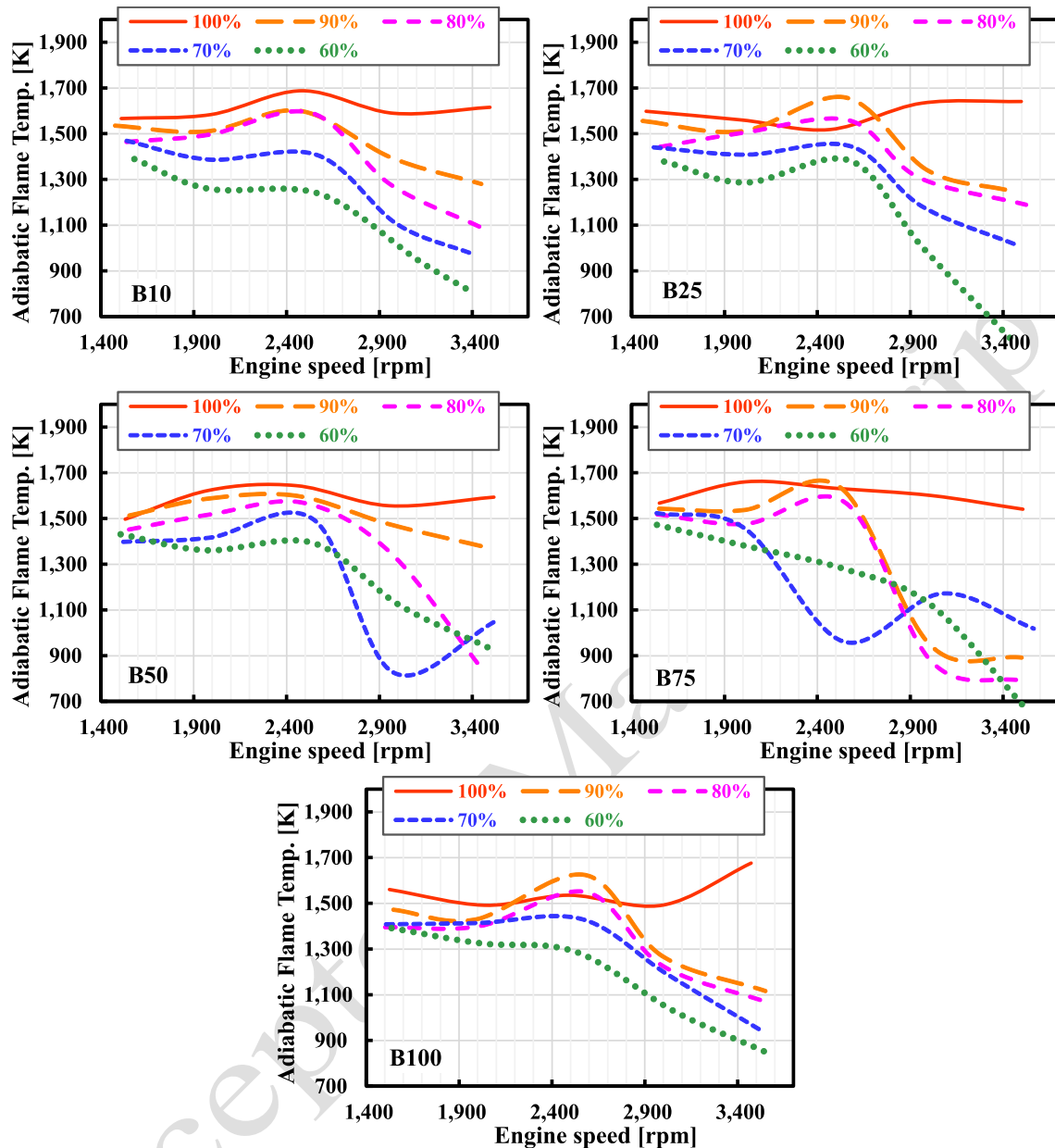


Figure 7. Adiabatic flame temperature for each operating point and blend

4. Conclusions

The physical and chemical properties of the different blends were determined, and the following conclusions were drawn:

The cetane index of pure Biodiesel (B100) is 17% higher than that of commercial fuel, which can have a positive effect on the start of the combustion process by reducing the delay time. According to other studies, it induces higher combustion pressures and temperatures, increasing the formation of NO_x emissions.



A regression was statistically determined for density and viscosity as a function of fuel percentage and temperature. The coefficients statistically represent the fit equation with a normal deviation of the residuals of 0.70 and 0.12, respectively.

It was proven that the viscosity obtained experimentally decreases as the temperature increases exponentially, according to theory.

The combustion temperature ranges at all load degrees, and operating regimes remain between 800 K and 1,700 K, with slight differences in their behavior as the rotation regime increases for the different blends.

5. Declaration of competing interest

We declare that we have no significant competing interests including financial or non-financial, professional, or personal interests interfering with the full and objective presentation of the work described in this manuscript.

6. Acknowledgments

The researchers are grateful to BioD S.A. company for having contributed to the development of this research project, delivering the fuel necessary for the tests and for their collaboration in determining the biofuel content of each sample. Finally, thanks to Escuela Colombiana de Ingeniería Julio Garavito and La Fundación Universitaria Los Libertadores for their support to the project.

7. Funding

This work was supported by Universidad Escuela Colombiana de Ingeniería Julio Garavito and La Fundación Universitaria Los Libertadores.

8. Author contributions

O.Venegas and L.F. Mónico carried out the experiment and wrote the paper. O. Venegas performed the statistical analysis. All authors discussed the results and contributed to the final manuscript.

9. Data availability statement

The authors confirm that the data supporting the findings of this study are available within the article

References

- [1] A. B. B. P. y. L. M. A.J. Torregrosa, "Impact of Fischer-Tropsch and biodiesel fuels on trade-offs between pollutant emissions and combustion noise in diesel engines," *Biomass and Bioenergy*, no. 52, p. 13, 2013.



- [2] T. D. R. L. a. B. Z. Prvulovic Slavica, "ANALYSIS OF STATE IN BIODIESEL PRODUCTION IN SERBIA," *Journal of Applied Engineering Science*, vol. 7, pp. 61 - 66, 2009.
- [3] A. Diaz Burgos, J. J. Lozada Castro, C. A. Castillo Parra, P. Fernandez Izquierdo and D. Arturo Perdomo, "Obtaining Biodiesel from Fat Extracted from Solid Waste Produced in the Fleshing Stage of Leather Manufacturing," *Ingeniería e Investigación*, vol. 43, p. e97254, November 2022.
- [4] R. P. Imbaquingo Navarrete, A. F. Cevallos González and C. Mafla Yépez, "Disminución de la opacidad en las emisiones de gases contaminantes en motores de encendido por compresión mediante el uso de biodiésel B5 y B10 a base de algas (chlorella)," *Ingeniería y Desarrollo*, vol. 38, p. 212–223, 2020.
- [5] L. F. M. Muñoz, *Contribución al estudio del ruido de Combustión en Conceptos Avanzados de Combustión Diesel*, Valencia - España, 2013.
- [6] J. Agudelo, P. Benjumea and A. P. Villegas, "Evaluation of nitrogen oxide emissions and smoke opacity in a HSDI diesel engine fuelled with palm oil biodiesel," *Revista Facultad de Ingeniería Universidad de Antioquia*, p. 62–71, 2010.
- [7] V. Kolanjiappan, "Reduction of amine and biological antioxidants on NOx emissions powered by mango seed biodiesel," *Revista Facultad de Ingeniería Universidad de Antioquia*, p. 46–54, 2017.
- [8] R. Pereira, I. da Silva and J. Pardal, "Energy and Exergy Analysis in a Centrifugal Pump Driven by a Diesel Engine Using Soybean Biodiesel and Mixtures with Diesel," *Ingeniería e Investigación*, vol. 42, p. e88228, February 2022.
- [9] D. L. Blanco-Estupiñan, A. Bermudez-Castañeda and S. Marquez, "Performance of Nozzle Steels in Biofuel," *Ingeniería y Universidad*, vol. 26, July 2022.
- [10] Fedebiocombustibles, 14 07 2023. [Online]. Available: <https://fedebiocombustibles.com/statistics/#>. [Accessed 14 07 2023].
- [11] Fedebiocombustibles, 2019a. [Online]. Available: <http://www.fedebiocombustibles.com/nota-web-id-147.htm>. [Accessed 06 11 2019].
- [12] Fedebiocombustibles, 2019b. [Online]. Available: <http://www.fedebiocombustibles.com/nota-web-id-177.htm>. [Accessed 06 11 2019].
- [13] Fedebiocombustibles, 2019c. [Online]. Available: <http://www.fedebiocombustibles.com/nota-web-id-195.htm>. [Accessed 06 11 2019].
- [14] Ministerio de Minas y Energía, 2019. [Online]. Available: <http://www.fedebiocombustibles.com/nota-web-id-621.htm>.



- [15] I. o. B. b. p. i. C. o. a. D. Engine, "O. Venegas and L.F. Mónico," *JOURNAL OF MECHANICAL ENGINEERING AND SCIENCES (JMES)*, vol. 15, pp. 8428 - 8439, 2021.
- [16] A. A. Espitia-Cubillos, A. E. Delgado-Tobón and S. A. Camargo-Vargas, "Estimación teórica del efecto de la temperatura en la densidad, viscosidad, poder calorífico, capacidad calorífica y gravedad API de biocombustibles," *Scientia et Technica*, vol. 24, no. 02, pp. 190 - 199, 2019.
- [17] G. C. y. C. V. Pedro N. Benjumea, "Efecto de la temperatura sobre la densidad del Biodiesel de aceite de palma y sus mezclas con Diesel convencional.," *Revista Energética*, no. 36, p. 10, 2006.
- [18] Á. M. Á. y. A. P. M. Pedro N. Benjumea, "Predicción del efecto de la temperatura sobre la viscosidad del biodiesel de aceite de palma y sus mezclas con diesel convencional.," *Revista Energética*, no. 35, p. 7, 2006.
- [19] A. R. Martinez, *Calculo de las Propiedades Fisicoquímicas Del Biodiesel y sus Mezclas Con Diesel A Partir De Reglas De Mezclado*, Cartagena - Colombia, 2013.
- [20] K. L. (. Poma Flores, *EVALUACIÓN DE LA CALIDAD DEL DIESEL*, Lima.
- [21] K. W. K. S. N. S. O. S. Noel Bezaire, "Limitations of the use of cetane index for alternative compression ignition engine fuels," *Fuel*, vol. 89, p. 3807–3813, 2010.
- [22] W. Klopfenstein, "Estimation of Cetane Index for Esters of Fatty Acids," *JAACS*, vol. 59, no. 12, pp. 531 - 533, 1982.
- [23] J. Rodríguez Fernández, *Estudio Bibliográfico y Experimental de las Emisiones y Prestaciones de un Motor Trabajando con Biodiesel*, Universidad de Castilla la Mancha, 2008.
- [24] ASTM, *ASTM D976 Standard Test Methods for Calculated Cetane Index of Distillate Fuels.*, 2011.
- [25] Ayuntamiento de Zaragoza., *Tablas de Poder Calorífico.*, Zaragoza: Ingemecanica, 2019.
- [26] P. Szymkowicz, "Analytical and experimental investigation of multi-component surrogate diesel fuels," Valencia, 2017.
- [27] Z. Luo, S. Som, S. M. Sarathy, M. Plomer, W. J. Pitz, D. E. Longman and T. Lu, "Development and validation of an n-dodecane skeletal mechanism for spray combustion applications," *Combustion Theory and Modelling*, vol. 18, pp. 187-203, 2014.
- [28] K. Narayanaswamy, P. Pepiot and H. Pitsch, "A chemical mechanism for low to high temperature oxidation of n-dodecane as a component of transportation fuel surrogates," *Combustion and Flame*, vol. 161, pp. 866-884, 2014.
- [29] H. Kahila, A. Wehrfritz, O. Kaario and V. Vuorinen, "Large-eddy simulation of dual-fuel ignition: Diesel spray injection into a lean methane-air mixture," *Combustion and Flame*, vol. 199, pp. 131-151, 2019.



- [30] Y. Pei, M. Mehl, W. Liu, T. Lu, W. Pitz and S. Som, "A Multi-Component Blend as a Diesel Fuel Surrogate for Compression Ignition Engine Applications (ICEF2014-5625)," *Journal of Engineering for Gas Turbines and Power*, vol. 137, 11 2015.
- [31] C. J. Mueller, W. J. Cannella, T. J. Bruno, B. Bunting, H. D. Dettman, J. A. Franz, M. L. Huber, M. Natarajan, W. J. Pitz, M. A. Ratcliff and K. Wright, "Methodology for Formulating Diesel Surrogate Fuels with Accurate Compositional, Ignition-Quality, and Volatility Characteristics," *Energy & Fuels*, vol. 26, pp. 3284-3303, 2012.
- [32] R. F. R. B. A. M. M. Glaude, "Adiabatic flame temperature from biofuels and fossil fuels and derived effect on NOx emissions," *Fuel Proc. Technol*, pp. 229-235, 210.
- [33] NIST, *Standard Reference Data Program*, 2019.
- [34] D. Ballerini, LES BIOCARBURANTS-Répondre aux défis énergétiques et environnementaux des transports, IFP, Ed., Editions TECHNIP, Paris, France, 2011.
- [35] J. E. Dec and R. E. Canaan, "PLIF Imaging of NO Formation in a DI Diesel Engine1," in *SAE Technical Paper*, 1998.
- [36] R. Amorim, "COMBUSTIÓN POR DIFUSIÓN DE BAJA TEMPERATURA EN MOTORES DIESEL DE PEQUEÑA CILINDRADA," 2010.
- [37] J. Benajes, S. Molina, R. Novella and R. Amorim, "Study on Low Temperature Combustion for Light-Duty Diesel Engines," *Energy & Fuels - ENERG FUEL*, vol. 24, 12 2009.
- [38] A. Sarangi, "Diesel low temperature combustion: an experimental study," 8 2012.
- [39] K. Kannan, "AN EXPERIMENTAL INVESTIGATION OF LOW TEMPERATURE COMBUSTION REGIMES IN A LIGHT DUTY ENGINE," 2016.
- [40] B. Tompkins, "The Characterization of Two-Stage Ignition Effects on Late Injection Low Temperature Combustion Using Biodiesel and Biodiesel Blends," 2015.